



Finite element analysis of web crippling failure of cold-formed steel members: modeling recommendations based on a review of best practices

Vitaliy V. Degtyarev¹, Helen Chen², Cristopher D. Moen³, Kara D. Peterman⁴, Benjamin W. Schafer⁵, Shahabeddin Torabian⁶, Shangqun Zhou⁷

Abstract

Large depth-to-thickness ratios of cold-formed steel (CFS) member webs can cause web crippling instabilities, which can be the critical limit state in design. Modern design standards contain provisions for web crippling strength calculations of the most common CFS members used in North American construction. However, for members outside of the standards, physical testing has historically been required to assess their web crippling capacity. Multiple publications describing successful applications of finite element (FE) analysis for simulating the web crippling behavior of CFS members indicate that FE analysis is a viable alternative for physical testing when appropriate FE modeling techniques are used. The presented study proposes recommendations for FE modeling of web crippling of various CFS member types, including those with web perforations and longitudinal web stiffeners, based on an extensive literature review and identified best practices. The recommendations address all aspects of the modeling and analysis, such as analysis type, element type, mesh density, material modeling, boundary conditions, loading, and others.

1. Introduction

Web crippling is a failure mode of cold-formed steel (CFS) members subjected to concentrated loads or reactions. It involves a nonuniform stress distribution in the web, web bending due to the load eccentricity caused by the rounded corners, web buckling, and local yielding (Sivakumaran 1989; Natário et al. 2014b; Yu et al. 2019). These factors make developing analytical models for predicting the web crippling strength extremely challenging. Therefore, the North American design specification (AISI S100-16 w/S2-20 2020) provides an empirical equation for determining the web crippling strength, developed based on an extensive test database. The equation considers the steel thickness, yield stress, corner radius, web height and angle, and bearing length as factors

¹Design and Research Engineer, New Millennium Building Systems, LLC, <vitaliy.degtyarev@newmill.com>

²Manager, Construction Standards Development, AISI, <hchen@steel.org>

³Owner, RunToSolve, LLC, <cris.moen@runtosolve.com>

⁴Associate Professor, Department of Civil and Environmental Engineering, University of Massachusetts Amherst <kdpeterman@umass.edu>

⁵Professor, Department of Civil and Systems Engineering, Johns Hopkins University <schafer@jhu.edu>

⁶Senior Consulting Engineer, Simpson Gumpertz & Heger Inc. <storabian@sgh.com>

⁷Graduate Student, Department of Civil and Systems Engineering, Johns Hopkins University <szhou71@jhu.edu>

affecting the web crippling strength and includes four empirical coefficients, which depend on the structural member type, support condition, and load case. The AISI S100 equation can only be used for the specific ranges of the variables presented in the specification. Physical testing in accordance with AISI S909 (2017) is required for structural members outside the AISI S100 limitations.

Powerful computational methods and resources are currently available, making numerical simulations an attractive alternative for physical testing. However, numerical models must include certain features and be appropriately validated to produce accurate results. Many researchers have successfully used the finite element (FE) analysis method to simulate web crippling tests and presented FE model parameters that allowed them to achieve good results since 1989 when Sivakumaran (1989) published the first paper on this topic. The goals of this study were to review publications describing FE modeling of the web crippling failure to identify the most important FE model parameters for achieving accurate results and develop a FE modeling protocol for web crippling test simulations, which also addresses the appropriate methods of model validation and resistance factor determination. The simulation-based determination of the web crippling strength in accordance with the proposed modeling protocol is recommended as an alternative for the physical testing within the AISI S100 (2020) framework.

2. Review of FE Simulations Reported in the Literature

A literature survey identified 48 publications describing FE modeling of web crippling failure of CFS members, which span from 1989 to 2022 and cover a wide range of CFS sections, section features, and loading conditions, as discussed hereafter. The publications on cold-formed stainless steel members were not considered because they are beyond the scope of AISI S100 (2020). It should also be noted that some papers described model validation for one condition and parametric studies using the validated models for slightly different conditions. For example, Fang et al. (2021) validated FE models of lipped channels with web openings using experimental data for ambient temperatures and performed a parametric study on the developed models for elevated temperatures. Gatheeshgar et al. (2021) validated models on test results for lipped channels with solid webs and large web openings and used the models in a parametric study of lipped channels with staggered slotted web perforations. Dwivedi and Vyavahare (2022) validated FE models on lipped channels and performed a parametric study on the models for lipped Z-sections. In such cases, only the models validated on test results were considered in the following analysis.

The first paper on the FE simulation of web crippling behavior of CFS members was published in 1989 (Sivakumaran 1989). It describes FE analysis of lipped channels under interior one-flange (IOF) loading in ADINA software. Despite simplifications used in the models due to the limited computational resources available then, reasonable agreement with the test results was achieved (the mean and coefficient of variation (CoV) of the test-to-prediction ratios were 1.01 and 0.125, respectively, for three samples). The second paper on this topic was published 13 years later, in 2002, by Hofmeyer et al. (2002), where the combined web crippling and bending moment failure of CFS deck sections under IOF loading was analyzed in ANSYS. From 2002 to 2016, up to two studies on the considered topic were published each year, whereas recent years have seen an increased number of publications, with four to eight studies published each year.

Abaqus, ANSYS, ADINA, and LUSAS software were used for the FE simulations of the web crippling failure in 32 (69%), 13 (27%), 1 (2%), and 1 (2%) publications, respectively.

Fig. 1 presents the percentages of CFS section types, section features, and loading conditions considered in the publications (see the Nomenclature section for abbreviation definitions). The evaluated loading conditions are illustrated in Fig. 2. It should be noted that some publications described FE simulations of several sections, section features, and loading conditions, resulting in the total number of considered cases (119) greater than the number of publications (48).

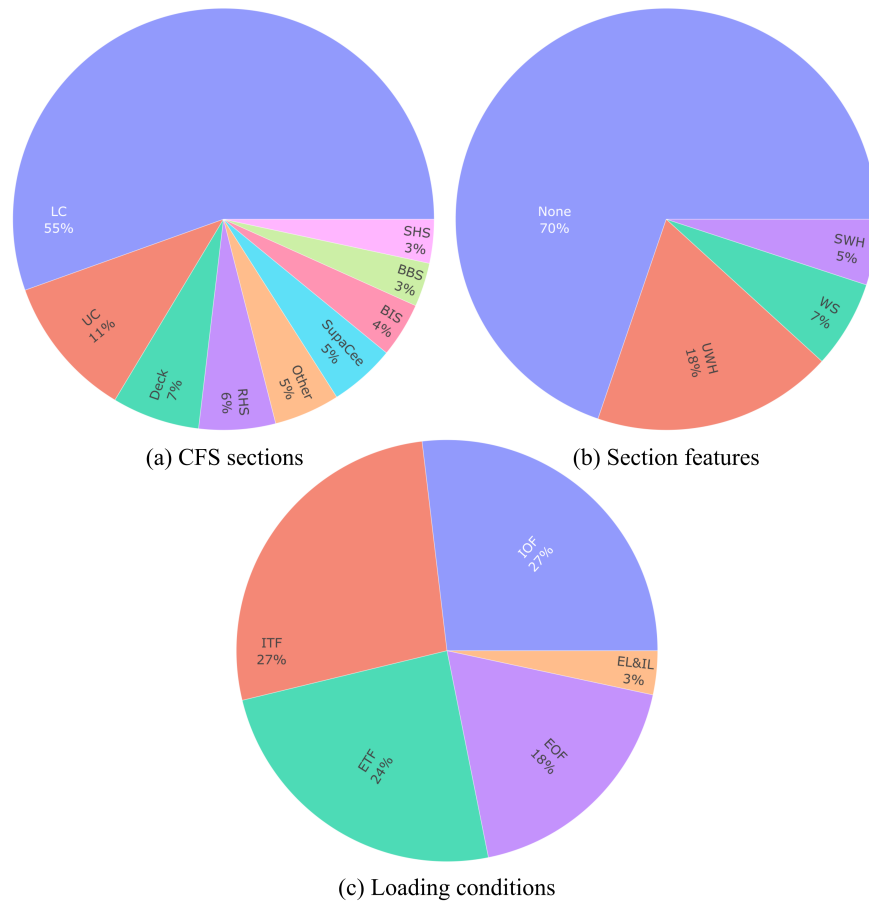


Figure 1: CFS sections, section features, and loading conditions considered in the literature

Fig. 1(a) shows that lipped channels (LC) received the most significant attention from researchers, with 55% of the evaluated cases investigating LC. Unlipped channels (UC), deck sections, rectangular hollow sections (RHS), SupaCee sections, and other sections (LiteSteel beams (LSB), lipped Z- and Sigma sections, and cassettes) were modeled in 11, 7, 6, 5 and 5% of the cases, respectively. They were followed by built-up I-sections (BIS) (4%), built-up box sections (BBS) (3%), and square hollow sections (SHS) (3%).

The section features considered in the literature are related to the section webs and include none (plain webs with no holes or stiffeners), unstiffened web holes (UWS), stiffened web holes (SWS), and longitudinal web stiffeners (WS) (see Fig. 1(b)). The vast majority of the publications presented FE models for plain webs (70%), followed by UWH (18%), WS (7%), and SWH (5%). The

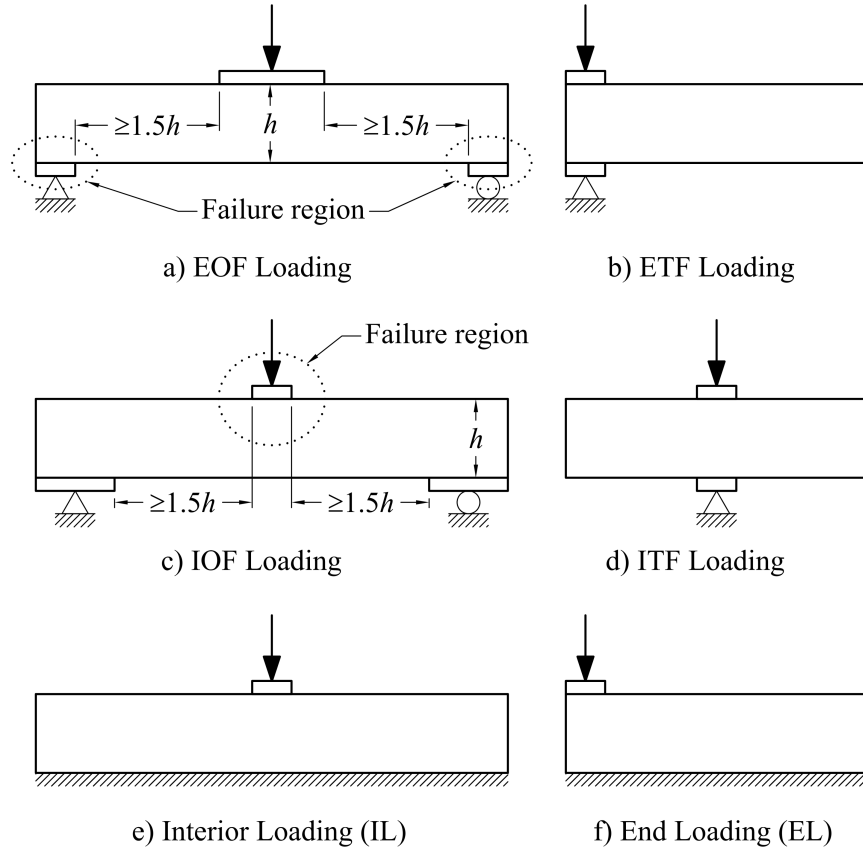


Figure 2: Web crippling loading conditions

considered loading conditions covered IOF (27%), ITF (27%), ETF (24%), EOF (18%), and EL and IL (3%) (see Figs. 1(c)) and 2). It should be noted that the EL and IL loading conditions are not specified in AISI S100 (2020) but were modeled by Li and Young (2019a) and He and Young (2022a) to simulate loading conditions of floor joists. FE models of high-strength CFS members were described in eight papers (Akhand et al. 2004; Gatheeshgar et al. 2021, 2022; Kanthasamy et al. 2022a, 2022b; Li and Young 2018, 2019a, 2019b), whereas the remaining papers dealt with normal strength steel.

All authors reported good agreement of the FE simulation results with experimental data. Table 1 summarizes model validation results presented in 37 reviewed publications. The publications not listed in Table 1 referenced previously published papers already considered in the review, compared load-displacement curves from the tests and simulations, or presented the mean and CoV values of the FEA-to-test ratios, which were impossible to convert into those for the test-to-FEA ratios without the ratios presented for each validated model. Some authors published model validation results for different cases separately (Elilarasi and Janarthanan 2020; Elilarasi et al. 2020; Fang et al. 2021; Gatheeshgar et al. 2021, 2022; Hareindirasarma et al. 2021; Heurkens et al. 2018; Janarthanan et al. 2019a; Li and Young 2018, 2019a; Lian et al. 2016, 2017; Macdonald et al. 2011; Natário et al. 2017; Ren et al. 2006; Sundararajah et al. 2017, 2018, 2019; Uzzaman et al. 2012, 2017, 2020a, 2020b). In those cases, the mean and CoV values of the test-to-FEA ratios were combined through the weighted mean and combined variance (Agarwal 2006). Overall, Table 1

shows 1,467 validation cases for various sections and loading conditions, with the combined mean and CoV values of 1.00 and 0.077, respectively.

Table 1: Summary of FE model validation results reported in the literature

Reference	Section	Strength	Loading	Validation Results		
				No.	Test/FEA Mean	CoV
Almatrafi et al. (2021)	Sigma	WC	IOF	6	0.96	0.080
Chen et al. (2021)	LC	WC	ETF, ITF	36	0.99	0.070
Dwivedi and Vyavahare (2022)	LC	WC	ETF	6	1.00	0.021
Elilarasi et al. (2020)	UC	WC	ETF	22	0.99	0.055
Elilarasi and Janarthanan (2020)	LSB, LC, UC	WC	ETF	115	1.05	0.090
Fang et al. (2021)	LC	WC	IOF	61	0.97	0.052
Gatheeshgar et al. (2021)	LC	WC	EOF	37	0.99	0.076
Gatheeshgar et al. (2022)	LC	WC	IOF	17	1.05	0.038
Hareindirasarma et al. (2021)	LC, LSB	WC	ITF	24	1.03	0.059
He and Young (2022a)	BIS	WC	ETF, ITF, EL, IL	51	0.99	0.052
He and Young (2022b)	BBS	WC	EOF, IOF, ETF, ITF	35	1.00	0.049
Heiyanthuduwa (2008)	LC	WC	EOF, IOF, ETF, ITF	108	1.03	0.094
Heurkens et al. (2018)	LC	WC	EOF, IOF	36	1.01	0.057
Hofmeyer et al. (2022)	Deck	WC	IOF, ITF	73	0.98	0.070
Janarthanan et al. (2019a)	UC	WC	EOF, IOF	27	1.00	0.065
Kaitila (2004)	Cassettes, Deck	WC, M&WC	IOF, ITF	6	1.02	0.032
Kanthsamy et al. (2022a)	UC	WC	ETF	10	1.00	0.020
Kanthsamy et al. (2022b)	UC	WC	EOF	10	0.99	0.060
Li and Young (2018)	SHS, RHS	WC	EOF, IOF, ETF, ITF	57	1.04	0.090
Li and Young (2019a)	RHS	WC	EL, IL	37	0.97	0.054
Li and Young (2019b)	RHS	M&WC	IOF	28	1.00	0.048
Lian et al. (2016)	LC	WC	EOF	74	0.98	0.045
Lian et al. (2017)	LC	WC	IOF	61	1.01	0.024
Macdonald et al. (2011)	LC	WC	EOF, ETF	36	0.99	0.102
McIntosh et al. (2022)	LC	WC	ITF	6	1.03	0.028
Natário et al. (2017)	BIS, LC, UC, LZ	WC	ITF	130	0.97	0.094
Ren et al. (2006)	UC	WC	EOF, IOF	22	1.07	0.066
Sivakumaran (1989)	LC	WC	IOF	3	1.01	0.125
Sundararajah et al. (2017)	LC	WC	ETF, ITF	36	1.01	0.079
Sundararajah et al. (2018)	SupaCee	WC	EOF, IOF	42	1.10	0.065
Sundararajah et al. (2019)	LC	WC	EOF, IOF	36	1.05	0.076
Uzzaman et al. (2020a)	LC	WC	ETF	36	1.00	0.046
Uzzaman et al. (2020b)	LC	WC	ITF	36	1.01	0.025
Uzzaman et al. (2012)	LC	WC	ETF, ITF	82	0.96	0.043
Uzzaman et al. (2013)	LC	WC	ETF	25	0.98	0.050
Uzzaman et al. (2017)	LC	WC	EOF, IOF	36	0.99	0.017
Willems et al. (2021)	Deck	M&WC	IOF	4	0.90	0.104

The FE model validation results in Table 1 indicate that FE simulations of web crippling failure can achieve an excellent agreement with tests when appropriate modeling techniques are used. The following subsections discuss those techniques, including FE type and mesh, steel material modeling, boundary conditions and loading, contact definition, initial geometric imperfections, residual stresses, and analysis type.

2.1 FE Type and Mesh Density

Four-node shell elements were used for modeling CFS sections in 45 out of 48 reviewed publications, whereas 8-node elements were employed by Akhand et al. (2004) and Chen et al. (2015) and 16-node shell elements were selected by Sivakumaran (1989). The loading and supporting steel plates, when they were used (see subsection 2.4), were modeled with rigid shell, rigid solid, or solid elements. He and Young (2022a, 2022b) also reported the use of solid elements for modeling screws connecting channel webs in built-up I-sections, whereas Natário et al. (2017) applied tie constraints to simulate the fasteners of built-up I-sections.

All reviewed publications emphasized the importance of fine mesh in the web crippling failure regions, especially for the rounded corners when load and support bearing plates and the contact between the plates and CFS members were modeled explicitly. Fine discretization of rounded corners is vital for capturing the progressive plastic deformation of the corners and changes in contact conditions under the increasing concentrated load or reaction (Hofmeyer 2005).

In the reviewed publications, some researchers indicated that the corners at the web crippling failure locations were discretized with 7 to 20 elements, while others stated that the element size along the arc was 0.5 or 1 mm. Some publications pointed out that a finer mesh was specified for the loaded corners at the web-flange junction without providing further details. It should also be noted that the required mesh density at the corners appears to depend on the failure mode and CFS section type. Hofmeyer et al. were able to achieve a good agreement of the FE simulations with test results with only 2 to 4 corner elements for the yield arc and rolling failure modes of the deck (Hofmeyer et al. 2002; 2018), whereas they had to use 10 elements for the rolling yield eye failure mode (Hofmeyer et al. 2002). Elilarasi and Janarthanan (2020) reported that the corner radius has an insignificant effect on the web crippling strength in LiteSteel beams, which allowed them to use 3x3 mm elements for the entire model.

Flat portions of the members were modeled with 1- to 15-mm elements near the load or reaction and 2.5- to 22-mm elements away from the load. Some researchers used a uniform mesh for the entire member length (Almatrafi et al. 2021; Janarthanan et al. 2019b; Janarthanan and Mahendran 2020), while others specified a finer mesh in the loaded region and coarser mesh elsewhere (Heiyanthuduwa 2008; Macdonald et al. 2006; Macdonald and Heiyantuduwa 2012; Natário et al. 2014a). A finer mesh was also used near openings when web-perforated members were studied (B. Chen et al. 2021; Uzzaman et al. 2013). The bearing plates were typically discretized with 5- to 10-mm elements, but a finer 2-mm mesh was also used (Hofmeyer et al. 2022; Willems et al. 2021; Zakhimi et al. 2020).

2.2 Steel Material Modeling

Von Mises yield criteria with isotropic hardening and bilinear or multilinear stress-strain curves were used for modeling CFS sections in the reviewed literature. Bilinear stress-strain curves with and without strain hardening were utilized. Janarthanan and Mahendran (2020) indicated that the web crippling capacity increased by only 2.8% when the elastic-perfectly plastic stress-strain diagram was replaced by a bilinear diagram with strain hardening. For multilinear stress-strain curves, engineering stresses and strains were converted into true stresses and strains using the EN 1993-1-5 (2006) equations.

The steel yield stress increase of the corners due to cold-forming was not considered in most publications, except for those authored by Kanthasamy et al. (2022a, 2022b) and Ren et al. (2006). Li and Young (2018, 2019a, 2019b) incorporated different stress-strain curves for the webs, flanges, and corners of hollow sections based on the measured stress-strain data. They also extended the corner properties by $2t$, where t is steel thickness, into the adjacent flat regions.

2.3 Boundary Conditions and Loading

Boundary conditions of the FE models in the reviewed literature simulated those in the physical tests used for the model validation. Some researchers imposed symmetry boundary conditions, where applicable, to reduce the computation time, while others analyzed full models. The concentrated loads were simulated in the models by vertical displacements imposed on the load bearing plates or directly on the CFS sections in practically all publications. Only earlier studies describe loading the models by pressure (Akhand et al. 2004; Sivakumaran 1989).

2.4 Contact Definition

Only three earlier publications (Sivakumaran 1989; Akhand et al. 2004; Ren et al. 2006) describe FE models with no load/support bearing plates and contact elements between them and CFS sections. Hofmeyer et al. (2002) used contact elements in the models for predicting the yield arc failure and did not use them for the yield eye failure of deck sections due to encountered solution convergence issues. All other publications describe surface-to-surface contact modeled via specifying contact pairs, which allowed for the separation of contact surfaces when the applied load increased. The corner elements not initially in contact with the load/support bearing plates were also included in the contact definition, as they eventually came into contact with the plates once significant localized deformations occurred. Natário et al. (2014a; 2014b; 2017) recommended separating the contact surfaces by a distance of $t/2$ to prevent initial surface over-closure. Several researchers followed this recommendation (Janarthanan et al. 2019a; Kanthasamy et al. 2022a, 2022b; Sundararajah et al. 2017, 2018, 2019; Elilarasi et al. 2020).

In the most reviewed publications, the normal contact behavior was modeled with the “hard” pressure-overclosure relationship, characterized by the assumptions of no penetration and no limit to the contact surface pressure magnitude, whereas the surface separation with no contact pressure was allowed. Natário et al. (2014a), Janarthanan et al. (2019a), and Sundararajah et al. (2017; 2019) investigated the effects of the “hard” and “softened” contact relationships on the simulation results. In the “softened” contact, the interpenetration of the surfaces (overclosure) was allowed, and the contact pressure linearly depended on the overclosure. They all found that the contact stiffness ranging from 2,000 to infinity (“hard” contact) insignificantly affected the ultimate load. Natário et al. (2014a) and Janarthanan et al. (2019a) reported smoother load-displacement curves obtained for the “softened” contact with contact stiffness of 4,000 and 10,000, respectively, whereas no difference in the curve smoothness was observed by Sundararajah et al. (2019).

Researchers used various values of the friction coefficient ranging from zero (frictionless contact) to 0.5 to simulate the tangential contact behavior and obtained good agreements with the experimental data (see Table 1). Natário et al. (2014a; 2014b) and Janarthanan et al. (2019a) studied the effect of the friction coefficient ranging from 0 to 0.8 on the web crippling strength, which was

found to be insensitive to the friction coefficient value, as long as it prevents the global twisting behavior (Natário et al. 2014a). Willems et al. (2021) also indicated that the friction coefficient value is not critical for obtaining accurate predictions.

2.5 Initial Geometric Imperfections

The consideration of initial geometric imperfections is usually required in the computational modeling of CFS members to obtain realistic post-buckling behavior and strength (Schafer and Peköz 1998; Schafer et al. 2010). However, the reviewed literature indicates that the web crippling strength is insensitive to imperfections unless the imperfection magnitude is comparable with the corner radius. Only He and Young (2022a), Hofmeyer et al. (2018), Kaitila (2004), and Sundararajah et al. (2017; 2019) included the initial geometric imperfections into the FE models. He and Young (2022a) used the measured imperfection magnitude and indicated that considering the imperfections was important to achieve more accurate simulations. Hofmeyer et al. (2018) reported that the imperfections were critical for the yield eye and yield arc-to-yield eye transition failure modes and not critical for the yield arc failure mode. Sundararajah et al. (2017; 2019) modeled the imperfections using the eigenvector field approach with the maximum imperfection amplitude of $d_1/150$ (d_1 is the web flat portion depth) and stated that the consideration of such imperfections had a marginal effect on the web crippling strength.

The initial geometric imperfections usually have an insignificant effect on the web crippling capacity because the load application eccentricity due to the corner radii is considerably greater than the imperfection magnitude. Natário et al. (2014a; 2014b) studied the effects of the imperfections with magnitudes of $0.1t$, $0.5t$, and $1.35t$ (where t is the steel thickness) on the web crippling capacity of channels. They found that the imperfection magnitude has a marginal effect on the capacity unless the imperfection magnitude is similar to the corner radius. This finding can explain the sensitivity of the web crippling strength from the imperfections in the He and Young (2022a) study, where the sections with corner radii smaller than the steel thickness were used, resulting in the imperfection magnitude-to-radius ratios up to 0.9. Janarthanan et al. (Janarthanan et al. 2019a) analyzed the web crippling strength of unlippped channels under the EOF and IOF loading modeled with $0.5t$ imperfections, which were greater than $d_1/150$ imperfections based on the manufacturing tolerances, and without imperfections. They found that the imperfections affected the web crippling capacity for the EOF and IOF load cases by 2% and 1%, respectively, which allowed them not to consider the geometric imperfections in the FE models.

2.6 Residual Stresses

None of the reviewed publications reported the consideration of the residual stresses and strains from the manufacturing process. Natário et al. (2014a; 2014b) studied the effect of the residual stresses estimated using the methodology proposed by Moen et al. (2008). They concluded that the common practice of assuming that the influence of residual stresses is offset by strength increase from cold-forming (Schafer et al. 2010) applies to FE modeling of the web crippling failure. Therefore, both effects can be ignored in the FE simulations. Natário et al. (2014a) also pointed out that the accurate modeling of the residual stresses requires the knowledge of many parameters related to the CFS manufacturing, which may affect the simulation results but are often unknown at the time of FE modeling. Janarthanan (2017) reported that preliminary studies showed that the effects

of the residual stresses on the web crippling capacity did not exceed 0.5%.

2.7 Analysis Type

Implicit static, implicit dynamic (quasi-static), and explicit dynamic (quasi-static) analyses were used by different researchers for FE simulations of the web crippling failure. The implicit analysis involves solving equations by iterations at each time step, while the explicit analysis solves equations directly, without iterations, which makes it computationally stable. The time steps in the implicit analysis may be large, whereas the explicit analysis requires very small time increments to obtain accurate solutions.

Several authors reported that the implicit analysis of web crippling failure might not converge for some models (Hofmeyer et al. 2002; Janarthanan et al. 2019a; Kaitila 2004; Kanthasamy et al. 2022a), making the explicit analysis an appealing option used by many researchers. However, the explicit analysis requires a small stable time increment directly proportional to the smallest FE length. Small corner elements required for the web crippling failure modeling result in small stable time increments and may slow down the analysis. To reduce simulation time, quasi-static analyses of the web crippling failure can be performed by artificially increasing the load application time, which is often referred to as load rate scaling, or artificially increasing the mass density of the elements, which is often referred to as mass scaling (Natário et al. 2014a; Natário et al. 2014b). The mass scaling technique was used by Janarthanan et al. (2019a) and Janarthanan and Mahendran (2020), whereas Kanthasamy et al. (2022b) and Sundararajah et al. (2017; 2019) did not apply load rate nor mass scaling.

3. Recommendations for FE Modeling of Web Crippling Strength and Behavior

The presented literature review allowed for developing the following recommendations for determining the web crippling strength of CFS flexural members via FE simulations. These recommendations are proposed as an alternative for the physical testing within the AISI S100 (2020) framework.

3.1 Scope

The recommendations provide guidance on performing FE simulations to determine the web crippling strength (resistance) of CFS flexural members. They apply to single-web, multiple-web, and built-up web sections, including those with web perforations and longitudinal web stiffeners, subjected to IOF, EOF, ITF, and ETF loading, as defined in AISI S100 (2020) and AISI S909 (2017).

3.2 FE Modeling

The FE model should include the investigated CFS member and load/support bearing plates with contacts defined between them. In FE simulations, special attention should be given to the following items:

- the selection of CFS member dimensions;
- the selection of the FE type and mesh density;
- the modeling of material properties;

- the modeling of boundary conditions and loading;
- the modeling of contact between loading/bearing plates and CFS member;
- the modeling of initial geometric imperfections and residual stresses;
- the selection of analysis type and software;
- the determination of failure load;
- the FE model validation.

3.2.1 CFS Member Dimensions

The nominal dimensions of the CFS member cross-section should be used in the analyses. The lengths of the CFS member and bearing plates should be taken in accordance with AISI S909 (2017).

3.2.2 FE Type and Mesh Density

Shell or solid elements suitable for large-rotation and large-strain nonlinear applications should be used to model CFS members. Although shell elements were used in all reviewed publications, solid elements are also acceptable because shell elements are simplifications of solid elements. The appropriate mesh density should be determined from a convergence study (mesh sensitivity analysis). Significant mesh refinement is recommended for corner radii and near web perforations for obtaining accurate simulation results. Deformable solid, rigid solid, and rigid shell elements are acceptable for modeling bearing plates. It is also acceptable to discretize bearing plates with larger elements than those used for the CFS member.

3.2.3 Material Properties

Nominal values of material properties should be used in the FE models. The modulus of elasticity and Poisson's ratio of steel should be taken as 29,500 ksi (203,000 MPa) and 0.30, respectively. The following stress-strain diagrams are acceptable for describing the material behavior of CFS: elastic-plastic without strain hardening, elastic-plastic with linear strain hardening, and nonlinear. The selection of the strain hardening modulus and the nonlinear stress-strain curve should be justified. When a nonlinear stress-strain curve is used, the engineering stresses and strains shall be converted into true stresses and strains as follows (EN 1993-1-5 2006):

$$\sigma_{true} = \sigma(1 + \varepsilon) \quad (1)$$

$$\varepsilon_{true} = \ln(1 + \varepsilon) \quad (2)$$

where σ and σ_{true} are engineering and true stresses, respectively; ε and ε_{true} are engineering and true strains, respectively.

3.2.4 Boundary Conditions and Loading

The model boundary conditions should correspond to the test specimen details described in AISI S909 (2017). Structural fasteners can be modeled with solid elements, linear or nonlinear spring elements, or by providing tie constraints between the corresponding nodes of the connected components. The use of symmetry boundary conditions is acceptable. The concentrated load should be simulated in the FE model by vertical displacement imposed on the load bearing plate.

3.2.5 Contact Definition

The contacts between the CFS member and bearing plates should be defined to allow for their separation under the applied load. The target elements (master surfaces) should be defined on

bearing plates, with the contact elements (slave surfaces) on the CFS member. The corner elements not in contact with bearing plates initially should also be included in the contact definition. The contact friction coefficient can be in the range of 0 to 0.4. Where applicable, appropriate contact between the webs of built-up members should also be included in the FE model.

3.2.6 Initial Geometric Imperfections and Residual Stresses

Although the literature review indicated that the web crippling strength is insensitive to the initial geometric imperfections for many sections, the imperfections should be included in the FE model unless their insignificant effect on the web crippling strength is justified. The web crippling strength of CFS sections with small corner radii might be sensitive to the initial geometric imperfections. Unless a more refined analysis of the geometric imperfections is performed, the initial geometric imperfections based on the buckling shape of the webs with the magnitude of $h/150$ (where h is the depth of flat web portion measured along the web plane, disregarding longitudinal intermediate stiffeners) should be used. The buckling shape of the webs should be determined from a buckling analysis preceding the nonlinear failure analysis. Applying the initial geometric imperfections only to the CFS member web(s) is acceptable. Residual stresses can be excluded from the FE model if the strength increase from cold-forming is not considered.

3.2.7 Analysis Type and Software

Implicit and explicit (quasi-static) analyses are acceptable. When the explicit (quasi-static) analysis is used, an appropriate load rate resulting in the kinetic-to-internal energy ratio after the initial loading stages not greater than 5% shall be selected. Mass scaling is acceptable for explicit (quasi-static) analysis. The software shall be suitable for performing physically and geometrically nonlinear FE analysis with contact modeling capabilities. The material and geometric nonlinearity shall be accounted for in the analysis.

3.2.8 Failure Load Determination

The failure load should be taken as the maximum load supported by the model but not greater than the load producing stresses and strains equal to the tensile stresses and ultimate strains, respectively, of the steel assumed in the FE model.

3.2.9 Model Validation

The FE modeling protocol should be validated by comparing the failure load from the FE simulation with failure loads from at least three physical tests performed on the same section type with similar cross-section dimensions and material properties subjected to the same loading type as those in the FE simulations. The failure modes from the FE analysis should be similar to those from the tests.

3.3 Data Evaluation

The nominal web crippling strength shall be taken as the failure load from the FE analysis for the IOF, ITF, and ETF loading and the support reaction at the failure location under the failure load for the EOF loading. The safety and resistance factors used in the design should be computed in accordance with Section K2.1 of AISI S100 (2020). The mean value of the professional factor, P_m , should be taken as the mean value of the test-to-simulation ratios from the model validation. The coefficient of variation of test results, V_P , should be taken as the coefficient of variation of the

test-to-simulation ratios from the model validation, but not less than 0.065. The number of tests, n , should be equal to the number of tests used for the model validation. The computed resistance factor shall not exceed the corresponding resistance factor specified in AISI S100 (2020) for the web crippling strength. Based on the validation results reported in the literature (see Table 1), an expected value of the resistance factor computed in accordance with Section K2.1 of AISI S100 (2020) is 0.90 when the proposed modeling protocol is followed.

3.4 Analysis Report

The analysis report should contain the input and output data in an amount required for a third party to reproduce the analyses, including, but not limited by, the following:

- the name of the engineer who performed or supervised the simulations;
- the objectives and purposes of the FE simulations;
- drawings of the CFS member(s) considered in the simulations with all relevant dimensions;
- the test setup assumed in the FE simulations with all relevant dimensions, including the length of bearing plates, the distance between them if applicable, and the details about fasteners used if applicable;
- the steel grade assumed in the FE simulations, as well as the nominal yield and tensile stresses and the ultimate elongation of the steel;
- the software and analysis type used for the FE analyses, including all analysis setups;
- the FE types and mesh densities used in the FE analyses;
- the material model used in the FE model;
- the boundary conditions and loading used in the FE model;
- contact definition details;
- the initial geometric imperfections and residual stresses used in the FE model;
- the information about the test data used for the model validation;
- the model validation results, including details on how the failure load or web crippling strength was determined, comparisons of the load-displacement curves and failure modes from the simulation and tests;
- FE simulation results for studied CFS member(s), including the load-displacement curves, stress and strain contour plots at the failure load, and images showing failure modes;
- the safety and resistance factor calculations.

4. Conclusions

This paper presented a review of 48 publications on FE simulations of the web crippling failure of CFS members. The publications span from 1989 to 2022 and cover many sections, including lipped and unlipped channels, decks, hollow sections, built-up sections, and others. CFS members with plain webs, longitudinal web stiffeners, and unstiffened and stiffened holes under various loading conditions were analyzed. All publications reported good agreements of the FE simulations with experimental data.

Most publications presented CFS members modeled with 4-node shell elements and load/support bearing plates idealized by rigid shell elements, with surface-to-surface contact defined between them. All publications stressed the importance of fine meshing of the CFS members in the web

cripling failure regions, especially for the rounded corners. Bilinear stress-strain curves with and without strain hardening and multilinear stress-strain curves with von Mises isotropic hardening were successfully used in the reviewed publications.

“Hard” contact was found acceptable in most cases, whereas some authors reported smoother load-displacement curves when the “hard” contact was replaced by “softened” contact with relatively high stiffness. The web crippling strength was found insensitive to the friction coefficient. The initial geometric imperfections affected the web crippling strength only when the imperfection magnitude was comparable with the corner radius. The effect of the residual stresses on the web crippling strength was found insignificant.

The recommendations for determining the web crippling strength of CFS flexural members via FE simulations developed based on the literature review are also presented. These recommendations are proposed as an alternative for the physical testing within the AISI S100 (2020) framework.

References

- Agarwal, B.L. (2006). *Basic statistics*. New Age International.
- AISI S100-16 w/S2-20 (2020). *North American Specification for the Design of Cold-Formed Steel Structural Members*. American Iron and Steel Institute, Washington, D.C.
- AISI S909-17 (2017). *Test Standard for Determining the Web Crippling Strength of Cold-Formed Steel Flexural Members*. American Iron and Steel Institute, Washington, D.C.
- Akhand, A.M., Wan Badaruzzaman, W.H., and Wright, H.D. (2004). “Combined flexure and web crippling strength of a low-ductility high strength steel decking: experiment and a finite element model”. *Thin-Walled Structures* 42(7), 1067–1082.
- Almatrafi, M., Theofanous, M., Bock, M., and Dirar, S. (2021). “Slenderness-based design for sigma sections subjected to interior one flange loading”. *Thin-Walled Structures* 158, 107194.
- Chen, B., Roy, K., Fang, Z., Uzzaman, A., Chi, Y., and Lim, J.B.P. (2021). “Web crippling capacity of fastened cold-formed steel channels with edge-stiffened web holes, un-stiffened web holes and plain webs under two-flange loading”. *Thin-Walled Structures* 163, 107666.
- Chen, Y., Chen, X., and Wang, C. (2015). “Experimental and finite element analysis research on cold-formed steel lipped channel beams under web crippling”. *Thin-Walled Structures* 87, 41–52.
- Dwivedi, R. and Vyavahare, A.Y. (2022). “Web crippling behavior of perforated cold-formed Z-sections under end-two-flange loading”. *Materials Today: Proceedings* 6, 615–621.
- Elilarasi, K., Kasthuri, S., and Janarthanan, B. (2020). “Effect of circular openings on web crippling of unlippped channel sections under end-two-flange load case”. *Advanced Steel Construction* 16(4), 310–320.
- Elilarasi, K. and Janarthanan, B. (2020). “Effect of web holes on the web crippling capacity of cold-formed LiteSteel beams under End-Two-Flange load case”. *Structures* 25, 411–425.
- EN 1993-1-5 (2006). *Eurocode 3: Design of steel structures - Part 1-5: General rules - Plated structural elements*. European Committee for Standardization, Brussels, Belgium.
- Fang, Z., Roy, K., Liang, H., Poologanathan, K., Ghosh, K., Mohamed, A.M., and Lim, J.B.P. (2021). “Numerical simulation and design recommendations for web crippling strength of cold-formed steel channels with web holes under Interior-One-Flange loading at elevated temperatures”. *Buildings* 11(12), 666.
- Gatheeshgar, P., Alsanat, H., Poologanathan, K., Gunalan, S., Degtyareva, N., and Hajirasouliha, I. (2022). “Web crippling behaviour of slotted perforated cold-formed steel channels: IOF load case”. *Journal of Constructional Steel Research* 188, 106974.
- Gatheeshgar, P., Alsanat, H., Poologanathan, K., Gunalan, S., Degtyareva, N., Wanniarachchi, S., and Fareed, I. (2021). “Web crippling of slotted perforated Cold-Formed Steel channels under EOF load case: Simulation and design”. *Journal of Building Engineering* 44, 103306.
- Hareindirasarma, S., Elilarasi, K., and Janarthanan, B. (2021). “Effect of circular holes on the web crippling capacity of cold-formed LiteSteel beams under Interior-Two-Flange load case”. *Thin-Walled Structures* 166, 108135.
- He, J. and Young, B. (2022a). “Behaviour of cold-formed steel built-up I-sections with perforated web under localized forces”. *Journal of Constructional Steel Research* 190, 107129.

- He, J. and Young, B. (2022b). “Web crippling of cold-formed steel built-up box sections”. *Thin-Walled Structures* 171, 108789.
- Heiyanthuduwa, M. (2008). “Web crippling behaviour of cold-formed thin-walled steel lipped channel beams”. Ph.D. Glasgow Caledonian University.
- Heurkens, R.A.J., Hofmeyer, H., Mahendran, M., and Snijder, H.H. (2018). “Direct strength method for web crippling— Lipped channels under EOF and IOF loading”. *Thin-Walled Structures* 123, 126–141.
- Hofmeyer, H. (2005). “Cross-section crushing behaviour of hat-sections (Part I: Numerical modelling)”. *Thin-walled structures* 43(8), 1143–1154.
- Hofmeyer, H., Geers, S.W.A., Snijder, H.H., and Schafer, B.W. (2022). “The Direct Strength Method for first generation trapezoidal steel sheeting under Interior One Flange and Interior Two Flange web crippling”. *Thin-Walled Structures* 180, 109795.
- Hofmeyer, H., Kerstens, J.G.M., Snijder, H.H., and Bakker, M.C.M. (2002). “Combined web crippling and bending moment failure of first-generation trapezoidal steel sheeting”. *Journal of Constructional Steel Research* 58(12), 1509–1529.
- Hofmeyer, H., Vervoort, E.M.C., Snijder, H.H., and Maljaars, J. (2018). “Representativeness of compressed flange behaviour for trapezoidal steel sheeting under combined web crippling and bending”. *Proceedings Eight International Conference on Thin-Walled Structures ICTWS 2018, July 24-27, 2018, Lisbon, Portugal*.
- Janarthanan, B., Mahendran, M., and Gunalan, S. (2019a). “Numerical modelling of web crippling failures in cold-formed steel unlipped channel sections”. *Journal of Constructional Steel Research* 158, 486–501.
- Janarthanan, B., Sundararajah, L., Mahendran, M., Keerthan, P., and Gunalan, S. (2019b). “Web crippling behaviour and design of cold-formed steel sections”. *Thin-Walled Structures* 140, 387–403.
- Janarthanan, B. (2017). “Structural behaviour and design of cold-formed steel floor systems”. Ph.D. Queensland University of Technology.
- Janarthanan, B. and Mahendran, M. (2020). “Numerical study of cold-formed steel channel sections under combined web crippling and bending action”. *Thin-Walled Structures* 152, 106766.
- Kaitila, O. (2004). “Web crippling of cold-formed thin-walled cassettes”. Ph.D. Helsinki University.
- Kanthasamy, E., Alsanat, H., Poologanathan, K., Gatheeshgar, P., Corradi, M., Thirunavukkarasu, K., and Dissanayake, M. (2022a). “Web crippling behaviour of cold-formed high strength steel unlipped channel beams”. *Buildings* 12(3), 291.
- Kanthasamy, E., Chandramohan, D.L., Shanmuganathan, G., Poologanathan, K., Gatheeshgar, P., Corradi, M., and McIntosh, A. (2022b). “Web crippling behaviour of cold-formed high-strength steel unlipped channel beams under End-One-Flange load case”. *Case Studies in Construction Materials* 16, e01022.
- Li, H.-T. and Young, B. (2018). “Design of cold-formed high strength steel tubular sections undergoing web crippling”. *Thin-Walled Structures* 133, 192–205.
- Li, H.-T. and Young, B. (2019a). “Behaviour of cold-formed high strength steel RHS under localised bearing forces”. *Engineering Structures* 183, 1049–1058.
- Li, H.-T. and Young, B. (2019b). “Cold-formed high-strength steel tubular structural members under combined bending and bearing”. *Journal of Structural Engineering* 145(8), 04019081.
- Lian, Y., Uzzaman, A., Lim, J.B.P., Abdelal, G., Nash, D., and Young, B. (2016). “Effect of web holes on web crippling strength of cold-formed steel channel sections under end-one-flange loading condition – Part I: Tests and finite element analysis”. *Thin-Walled Structures* 107, 443–452.
- Lian, Y., Uzzaman, A., Lim, J.B.P., Abdelal, G., Nash, D., and Young, B. (2017). “Web crippling behaviour of cold-formed steel channel sections with web holes subjected to interior-one-flange loading condition-Part I: Experimental and numerical investigation”. *Thin-Walled Structures* 111, 103–112.
- Macdonald, M. and Heiyantuduwa, M.A. (2012). “A design rule for web crippling of cold-formed steel lipped channel beams based on nonlinear FEA”. *Thin-Walled Structures* 53, 123–130.
- Macdonald, M., Heiyantuduwa Don, M.A., Kotełko, M., and Rhodes, J. (2011). “Web crippling behaviour of thin-walled lipped channel beams”. *Thin-Walled Structures* 49(5), 682–690.
- Macdonald, M., Rhodes, J., and Heiyantuduwa, M.A. (2006). “Finite element analysis of web crippling behaviour of cold-formed steel”. *International Specialty Conference on Cold-Formed Steel Structures*. Orlando, Florida, U.S.A.
- McIntosh, A., Gatheeshgar, P., Gunalan, S., Kanthasamy, E., Poologanathan, K., Corradi, M., and Higgins, C. (2022). “Unified approach for the web crippling design of cold-formed channels: Carbon steel, stainless steel and aluminium”. *Journal of Building Engineering* 51, 104134.
- Moen, C.D., Igusa, T., and Schafer, B.W. (2008). “Prediction of residual stresses and strains in cold-formed steel members”. *Thin-Walled Structures* 46(11), 1274–1289.

- Natário, P., Silvestre, N., and Camotim, D. (2014a). “Computational modelling of flange crushing in cold-formed steel sections”. *Thin-Walled Structures* 84, 393–405.
- Natário, P., Silvestre, N., and Camotim, D. (2014b). “Web crippling failure using quasi-static FE models”. *Thin-Walled Structures* 84, 34–49.
- Natário, P., Silvestre, N., and Camotim, D. (2017). “Web crippling of beams under ITF loading: A novel DSM-based design approach”. *Journal of Constructional Steel Research* 128, 812–824.
- Ren, W.-X., Fang, S.-E., and Young, B. (2006). “Finite-element simulation and design of cold-formed steel channels subjected to web crippling”. *Journal of Structural Engineering* 132(12), 1967–1975.
- Schafer, B.W., Li, Z., and Moen, C.D. (2010). “Computational modeling of cold-formed steel”. *Thin-Walled Structures* 48(10-11), 752–762.
- Schafer, B.W. and Peköz, T. (1998). “Computational modeling of cold-formed steel: characterizing geometric imperfections and residual stresses”. *Journal of Constructional Steel Research* 47(3), 193–210.
- Sivakumaran, K.S. (1989). “Analysis for web crippling behaviour of cold-formed steel members”. *Computers & Structures* 32(3), 707–719.
- Sundararajah, L., Mahendran, M., and Keerthan, P. (2017). “New design rules for lipped channel beams subject to web crippling under two-flange load cases”. *Thin-Walled Structures* 119, 421–437.
- Sundararajah, L., Mahendran, M., and Keerthan, P. (2018). “Design of SupaCee sections subject to web crippling under One-Flange load cases”. *Journal of Structural Engineering* 144(12), 04018222.
- Sundararajah, L., Mahendran, M., and Keerthan, P. (2019). “Numerical modeling and design of lipped channel beams subject to web crippling under One-Flange load cases”. *Journal of Structural Engineering* 145(10), 04019094.
- Uzzaman, A., Lim, J.B.P., Nash, D., and Roy, K. (2020a). “Cold-formed steel channel sections under end-two-flange loading condition: Design for edge-stiffened holes, unstiffened holes and plain webs”. *Thin-Walled Structures* 147, 106532.
- Uzzaman, A., Lim, J.B.P., Nash, D., and Roy, K. (2020b). “Web crippling behaviour of cold-formed steel channel sections with edge-stiffened and unstiffened circular holes under interior-two-flange loading condition”. *Thin-Walled Structures* 154, 106813.
- Uzzaman, A., Lim, J.B.P., Nash, D., Rhodes, J., and Young, B. (2012). “Cold-formed steel sections with web openings subjected to web crippling under two-flange loading conditions—part I: Tests and finite element analysis”. *Thin-Walled Structures* 56, 38–48.
- Uzzaman, A., Lim, J.B.P., Nash, D., Rhodes, J., and Young, B. (2013). “Effect of offset web holes on web crippling strength of cold-formed steel channel sections under end-two-flange loading condition”. *Thin-Walled Structures* 65, 34–48.
- Uzzaman, A., Lim, J.B.P., Nash, D., and Young, B. (2017). “Effects of edge-stiffened circular holes on the web crippling strength of cold-formed steel channel sections under one-flange loading conditions”. *Engineering Structures* 139, 96–107.
- Willems, D.W.C., Hofmeyer, H., Snijder, H.H., and Schafer, B.W. (2021). “The direct strength method for combined bending and web crippling of second-generation trapezoidal steel sheeting”. *Thin-Walled Structures* 167, 108149.
- Yu, W.-W., LaBoube, R.A., and Chen, H. (2019). *Cold-Formed Steel Design*. 5th ed. John Wiley & Sons.
- Zakhimi, H., Hofmeyer, H., Snijder, H.H., and Mahendran, M. (2020). “Explicit and interaction direct strength methods for combined web crippling and bending moment failure of first-generation trapezoidal steel sheeting”. *Thin-Walled Structures* 157, 106927.

Nomenclature

BBS	Built-up box sections
BIS	Built-up I-sections
CoV	Coefficient of variation
EL	End loading
EOF	End one-flange loading
ETF	End two-flange loading
IL	Interior loading
IOF	Interior one-flange loading
ITF	Interior two-flange loading

LC	Lipped channels
LSB	LiteSteel beams
LZ	Lipped Z-sections
M&WC	Combined moment and web crippling
RHS	Rectangular hollow sections
SHS	Square hollow sections
SWH	Stiffened web holes
UC	Unlipped channels
UWH	Unstiffened web holes
WC	Web crippling
WS	Web stiffener